



## Membrane degradation in redox flow batteries

Felix Lulay, Claudia Weidlich, Markus Valtiner & Christian M. Pichler

To cite this article: Felix Lulay, Claudia Weidlich, Markus Valtiner & Christian M. Pichler (2023) Membrane degradation in redox flow batteries, Green Chemistry Letters and Reviews, 16:1, 2274529, DOI: [10.1080/17518253.2023.2274529](https://doi.org/10.1080/17518253.2023.2274529)

To link to this article: <https://doi.org/10.1080/17518253.2023.2274529>



© 2023 The Author(s). Published by Informa UK Limited, trading as Taylor & Francis Group



Published online: 25 Oct 2023.



Submit your article to this journal [↗](#)



Article views: 201



View related articles [↗](#)



View Crossmark data [↗](#)

## Membrane degradation in redox flow batteries

Felix Lulay<sup>a,c</sup>, Claudia Weidlich<sup>a</sup>, Markus Valtiner<sup>b,c</sup> and Christian M. Pichler<sup>b,c</sup>

<sup>a</sup>Team for Applied Electrochemistry, DECHEMA-Forschungsinstitut, Frankfurt am Main, Germany; <sup>b</sup>Institute of Applied Physics, Vienna University of Technology, Vienna, Austria; <sup>c</sup>Centre of Electrochemical and Surface Technology, Wiener Neustadt, Austria

### ABSTRACT

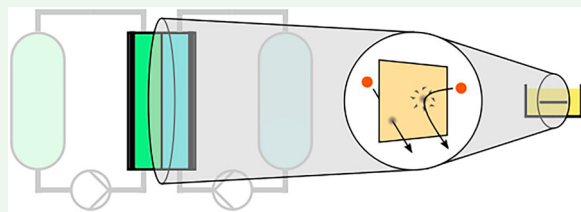
Redox flow batteries are a promising technology to enable the middle term storage of fluctuating renewable electricity production. The membrane is a key component in the battery system and to further develop and improve the battery systems, detailed understanding of the membrane aging and degradation mechanisms are required. This review gives a comprehensive overview about the various membrane degradation mechanisms in the most relevant redox flow battery systems. We discuss different testing approaches for membranes and compare the influence of different battery chemistries, testing protocols and degradation mechanisms. Based on the current state of the art, an outlook on the greatest challenges for developing novel and more stable membrane materials is given.

### ARTICLE HISTORY

Received 10 August 2023  
Accepted 18 October 2023

### KEYWORDS

Redox flow batteries;  
membranes; degradation  
mechanism; energy storage;  
polymer science





## Introduction

To reduce CO<sub>2</sub> emissions and curb the negative effects of climate change, fossil energy carriers shall be replaced by renewable, but intermittent energy sources like solar power and wind (1, 2). To still guarantee security of supply, buffer and grid balancing systems are needed in case of high discrepancies between supplied and demanded energy. Therefore, efficient and economically viable energy storage solutions are urgently required to balance the fluctuating nature of renewable electricity generation. These energy storage systems must be able to bridge different timescales, from seconds up to several weeks. Promising technologies especially for the middle term storage (hours to days) are redox flow batteries (RFBs) (3–5).

In RFBs the chemical energy is not stored in the electrode materials, but in the electrolyte, while the electrodes in the battery cell are solely used for the electrochemical conversion during charging and discharging. The electrolyte is stored in external tanks and pumped through the cell continuously, hence its amount is directly

proportional to the system's capacity and can be independently scaled from the power-determining size of the electrodes. The battery cell is divided into two half cells by an electrically isolating, ion-conducting membrane to prevent mixing of electrolyte, which would lead to self-discharge of the RFB. Depending on the wide range of possible electrolyte chemistries applied in RFBs, different membrane materials are available.

For RFB application, the membranes should exhibit high mechanical and chemical stability, a high permeation selectivity and conductivity for the charge-balancing ionic species (and therefore a low resistance) as well as an acceptable price. It is challenging to find an optimal material and often a trade-off between individual membrane properties has to be made. A crucial factor for economic feasibility is membrane aging and deactivation behavior. Because RFBs are part of an essential, long-lasting, low-maintenance energy storage infrastructure, it is of central interest to investigate the reasons and mechanisms for the degradation of main components, especially membranes. A schematic overview of a RFB is shown in Figure 1.

**CONTACT** Christian M. Pichler  christian.pichler@cest.at  CEST Centre of Electrochemical and Surface Technology, Viktor Kaplan Straße 2, Wiener Neustadt 2700, Austria

© 2023 The Author(s). Published by Informa UK Limited, trading as Taylor & Francis Group  
This is an Open Access article distributed under the terms of the Creative Commons Attribution-NonCommercial License (<http://creativecommons.org/licenses/by-nc/4.0/>), which permits unrestricted non-commercial use, distribution, and reproduction in any medium, provided the original work is properly cited. The terms on which this article has been published allow the posting of the Accepted Manuscript in a repository by the author(s) or with their consent.

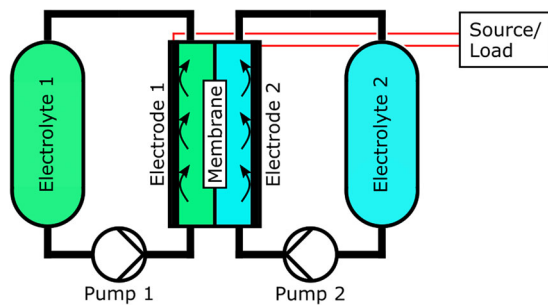
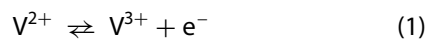


**Figure 1.** Schematic view of a RFB.

One of the most advanced RFB system to date is the all-vanadium RFB (VRFB) (6). VRFBs use an electrolyte with vanadium species of different oxidation states solvated in concentrated sulfuric acid. Vanadium is cycled between V(II) (charged state) and V(III) (discharged state) in the negative half cell (NHC) as shown in eq. (1) and between V(V) (charged state) and V(IV) (discharged state) in the positive half cell (PHC) as shown in eq. (2):



The discharge reaction is proceeding from left to right and charging from right to left. With a NHC standard potential of  $E_0^{-} = -0.26\text{V}$  and a PHC standard potential of  $E_0^{+} = 1.00\text{V}$  vs. the standard hydrogen electrode (SHE), a cell voltage of  $E_0 = 1.26\text{V}$  can be achieved (7). By employing vanadium as redox-active species in

**Table 1.** Possible pathways of membrane degradation and methods applicable to detect the resulting changes and defects.

Membrane deactivation mechanism	Causes, consequences, and detection methods
<b>Blockage</b> of membrane pores	<b>Due to</b> vanadium ions or contaminants <b>Leads to</b> decreased permeability/increased resistance, decreased voltaic efficiency <b>Detection with</b> optical assessment (if blocking species stains the membrane), permeability, resistance, and efficiency measurements
<b>Mechanical failure</b> of the membrane material	<b>Due to</b> polymer backbone degradation (e.g. oxidative decomposition) <b>Leads to</b> increased permeability/decreased resistance, sudden capacity/efficiency drops <b>Detection with</b> NMR spectroscopy/mass spectrometry (fragment analysis), SEM imaging, permeability, resistance, and efficiency measurements, mass loss, UV/Vis spectroscopy (e.g. of $\text{VO}^{2+}$ , if $\text{VO}_2^{+}$ is oxidizing the material)
<b>Pore degradation</b> inside the membrane	<b>Due to</b> functional group degradation/cleavage <b>Leads to</b> reduced ion exchange capacity <b>Detection with</b> XPS/vibrational spectroscopy (reduction of signal intensity for functional group), acid-base titration

both half cells, contamination by crossover through the membrane can be avoided. Nevertheless crossover takes place and leads to self-discharge of the VRFB (8–11). In addition to VRFBs, systems with other elements than vanadium have been developed such as the iron-chromium RFB (ICRFB), which employs the redox couples  $\text{Fe}^{2+}/\text{Fe}^{3+}$  and  $\text{Cr}^{2+}/\text{Cr}^{3+}$ , (5, 12) or the polysulfide bromine RFB with  $\text{S}_2^{2-}/\text{S}_4^{2-}$  and  $\text{Br}_3^{-}/\text{Br}^{-}$  as the redox-active species (13, 14). Additionally, interest in RFBs with metal-free electrolytes based on organic charge carriers like quinones or lignin based molecules arose. According to the different electrolyte chemistries various types (e.g. anion or cation exchanger) and compositions of membranes are available and amongst all RFB components (electrodes, current collectors, electrolyte etc.) the membrane plays a special role in the operation and performance of the battery. Degradation and malfunction of the membrane can lead to enhanced electrolyte crossover, increased cell resistance and even complete failure of the RFB system. Because of that, it is of great importance to gain an overview regarding the different membrane types applied in RFBs and their degradation mechanisms. Although there are several reviews dealing with general aging mechanisms in RFBs, there is only a small number of reviews discussing specifically the influence of membranes on the performance of the RFB, even though membranes contribute significantly to the overall system degradation. Most of those articles mainly focus on synthesis and the electrical characteristics of the membranes and only mention their degradation briefly (15, 16) or describe the membrane degradation just in a specific system, e.g. VRFBs or fuel cells (17, 18). A review giving an overview over the most important membrane materials used in the diverse RFB systems is still lacking.

Therefore, this review will discuss the various degradation mechanisms of RFB membranes, with different chemistry, structure and application range. A special focus will be laid on VRFBs, as they are the technically most mature system and are already used on an industrial scale. We will provide an overview on long-term aging mechanisms occurring during real-world battery stack operation and discuss *ex situ* methods for accelerated aging, to mimic and understand the mechanisms of those processes on a microscopic scale.

The degradation phenomena will be discussed for different types of membranes such as cation-exchange membranes (CEMs), anion-exchange membranes (AEMs) and non-ionic separators as well as composite and amphoteric membranes. Within the sections, the membranes are grouped by system and type.

The effects of aging show themselves as changes in measurable membrane properties such as resistivity, permeability, ion exchange capacity, weight, and swelling/thickness, as well as visually in form of stains and/or cracks. Hence, membrane degradation can be assessed based on these indicators (Table 1).

### Cation-exchange membranes

The most commonly applied CEM in RFBs is Nafion® (Dupont), a perfluorinated polymer with a polytetrafluoroethylene (PTFE) backbone and sulfonic acid-terminated perfluorovinyl ether groups to ensure proton conductivity (Figure 2) (19–22). Next to Nafion®, a variety of completely or partly fluorinated CEMs are applied in RFBs such as fumasep® membranes of Fumatech and Gore-Select®, a perfluorosulfonic acid (PFSA) polymer reinforced with PTFE, of Gore-Tex® (23–25). Additionally, non-fluorinated CEMs based on aromatic and aliphatic polymer backbones as well as composite CEMs are available.

### (Per)fluorinated membranes

#### VRFBs

A number of studies concluded that different Nafion® variants are generally stable in the sulfuric acid based vanadium electrolyte used for VRFBs (19, 24, 26, 27). Mohammadi and Skyllas-Kazacos investigated Nafion® 112 membranes soaked in  $\text{VO}_2^+$  solution regarding their change in mass, resistivity, and diffusivity as well as the amount of  $\text{VO}_2^+$  reduced to  $\text{VO}^{2+}$  in the process (26). The labeling of Nafion® membranes provides information about their properties: The first two assigned numbers describe the equivalent weight and the following numbers represent the thickness of the Nafion® membranes (in thousandths of an inch); Nafion® 112 and Nafion® 115 are e.g. 51 and 127  $\mu\text{m}$  thick,

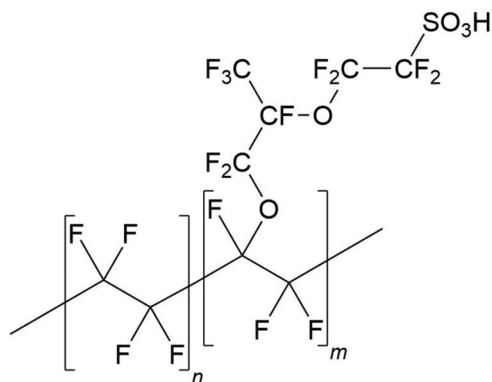


Figure 2. Structure of Nafion®.

respectively.  $\text{VO}_2^+$  was applied because of its oxidative properties, since the oxidative destruction of the membrane is a possible degradation pathway. After soaking the membrane in 0.1M  $\text{VO}_2^+$  solution for 60 days, there was no weight loss measurable despite 3% of  $\text{VO}_2^+$  was reduced to  $\text{VO}^{2+}$  as determined with ultraviolet/visible light (UV/Vis) spectroscopy.

In another set of experiments in the same study, Nafion® 112 was immersed into a 2M  $\text{VO}_2^+$  solution for 180 days. Afterwards, the membrane showed a 24% decrease in area-specific resistance as well as a 17% increase in diffusivity at a consistent ion exchange capacity (IEC). When the membrane was cycled in a VRFB at 30  $\text{mA}/\text{cm}^2$  for 180 days instead, resistivity strongly increased and diffusivity decreased, which was attributed to zinc (a contaminant in the electrolyte) and vanadium blocking the membrane channels. By soaking the membrane in sulfuric acid, this blockage could be reverted, as the Zn and V depositions causing the blockage are removed. In a similar study by Sukkar and Skyllas-Kazacos, Nafion® 112 was also treated with  $\text{VO}_2^+$  solution (24). The membrane was soaked in 0.1M  $\text{VO}_2^+$  solution for 120 days, where its resistivity decreased by 57% and its diffusivity increased by 237%. The larger changes compared to soaking in 2M  $\text{VO}_2^+$  solution was attributed to the increased membrane swelling in the diluted vanadium solution, making the pores more accessible for  $\text{VO}_2^+$ . The IEC of the soaked membrane also increased because of incorporation of anions such as sulfate and bisulfate ions during swelling. Additionally, a weight loss of 4.62% of the membrane was observed after 500 days of soaking in 0.1M  $\text{VO}_2^+$  solution. The oxidative degradation of the membrane was identified by reduction of  $\text{VO}_2^+$  to  $\text{VO}^{2+}$  measured using UV/Vis spectroscopy.

Xi *et al.* investigated the influence of temperature on the membrane degradation (27). They studied Nafion® 115 as well as Nafion® 212 at temperatures between  $-15^\circ\text{C}$  and  $50^\circ\text{C}$ . For the degradation tests, the respective membranes were cycled at 80  $\text{mA}/\text{cm}^2$  at  $-15^\circ\text{C}$ ,  $30^\circ\text{C}$ , and  $50^\circ\text{C}$ . Both Nafion® membranes demonstrate good stability and constant efficiencies over all temperature ranges. While reduced voltage efficiencies (VEs) were reported at  $50^\circ\text{C}$ , the limiting factor in this case was the electrolyte, from which  $\text{V}_2\text{O}_5$  precipitated, thereby disturbing the cycling process.

Vijayakumar *et al.* examined Nafion® 117 membranes cycled in VRFBs over a timespan of 3 days with UV/Vis spectroscopy, X-ray photoelectron spectroscopy (XPS), and nuclear magnetic resonance (NMR) spectroscopy (19). With UV/Vis spectroscopy, it was found that after removing the weakly attached vanadium species from the membrane surface *via* sonication, only  $\text{VO}^{2+}$  was

visible in the obtained spectra, which implies that only the vanadyl species adsorbs into the membrane channels. With  $^{19}\text{F}$  NMR, the fluorinated parts of fresh and cycled Nafion<sup>®</sup> membranes were compared, where no significant changes were observable, indicating a high chemical stability of the polymer.  $^{17}\text{O}$  NMR showed again only one vanadium species inside of the membrane, which was identified as  $\text{VO}^{2+}$  confirming the UV/Vis experiments. Also, the authors suggest that the  $\text{VO}^{2+}$  species inside the membrane do not form contact ion pairs with the sulfonic acid groups but bind *via* hydrogen bonds; they can also be removed from the membrane channels by treating the membrane with boiling water.

In addition to Nafion<sup>®</sup>, Sukkar and Skyllas Kazacos also investigated Gore-Select<sup>®</sup> membranes (Gore-Select<sup>®</sup> L-570, Gore-Select<sup>®</sup> L-01009, Gore-Select<sup>®</sup> L-01854, and Gore-Select<sup>®</sup> P-03430), which exhibit a similar pore structure (24). When soaked in 0.1M  $\text{VO}_2^+$  solution, the Gore-Select<sup>®</sup> membranes also exhibited a decreased resistivity (between 39% and 29% compared to 57% for Nafion<sup>®</sup> 112) and an increase in diffusivity (also lower as for the Nafion<sup>®</sup> membrane). The IEC increased similarly compared to Nafion<sup>®</sup> 112, however, the weight loss and spectroscopically observed  $\text{VO}^{2+}$  incorporation of the Gore-Select<sup>®</sup> samples was much lower.

Another PFSA CEM is Selemion<sup>®</sup> CMV (Asahi Glass Co.), which was tested by Mohammadi and Skyllas-Kazacos (26) as well as Xi *et al.* (27) Mohammadi and Skyllas-Kazacos immersed the CMV membrane in 0.1M  $\text{VO}_2^+$  solution for 60 days, during which a mass loss of more than 50% was observed and an according amount of  $\text{VO}^{2+}$  was measured photometrically, without suggesting a degradation mechanism for this observation. Xi *et al.* tested the CMV membrane among others in their VRFB setup, but excluded the material from temperature tests because of the

membrane's low capacity retention and VE, considering it as unsuitable for VRFBs. Hwang and Ohya also reported cracks in a CMV membrane after a durability test with 2M  $\text{VO}_2^+$  in 2M sulfuric acid after two months and noted that its resistance decreased. This effect was assigned to the creation of pinholes in the membrane, additionally indicating its degradation (28).

### Other aqueous RFBs

ICRFBs utilize Fe(II/III) and Cr(II/III) as redox pairs in an hydrochloric acid-based electrolyte. Sun *et al.* reported results regarding the stability of different membranes used in ICRFBs, including Nafion<sup>®</sup> 115 (22). While cycling data revealed an expectable drop in VE and energy efficiency (EE), the membrane was chemically stable. This was verified by an *ex situ* test soaking the membrane in a solution of 1M  $\text{Cr}^{3+}$  and 1M  $\text{Fe}^{2+}$  in 3M hydrochloric acid for 22 days, where the Nafion<sup>®</sup> membrane retained its dimensions as well as its weight.

In a study testing a range of redox-active molecules as charge carriers for RFBs published by Gao *et al.* the fouling tendencies of Nafion<sup>®</sup> 115 were investigated (29). The molecules (1) 1,1'-bis(propyl-3-trimethylammonium) ferrocene dichloride (BTMAP-Fc), (2) 1,1'-bis(propyl-3-sulfonate) ferrocene disodium salt (BSP-Fc), (3) methyl viologen (MV) and (4) anthraquinone-2,6-disulfonate (AQDS) were tested (all shown in Figure 3). The membrane was exposed to 0.1M active species in 1M aqueous NaCl solution and examined with galvanostatic intermittent titration technique (GITT) and electrochemical impedance spectroscopy (EIS). Gao *et al.* reported that the cationic redox-active species (BTMAP-Fc and MV) enter the Nafion<sup>®</sup> CEM readily in a setup with halfway charged electrolyte on each side of the membrane. In the EIS spectra, this manifests as enlarged capacitive arcs, while the *iR* drop measured with GITT increases as well over time. Optical assessment also showed a distinct color change of the previously transparent membrane. This blockage of the membrane by the redox-active species and the resulting electric field therefore hinders the exchange of ions for charge compensation during battery operation and is considered as fouling.

### Fuel cells

While fuel cells (FCs) have a similar schematic configuration as RFBs and use different types of polymeric membranes, they are a type of electrochemical energy converter on their own. Degradation mechanisms of membranes in FCs have been covered previously in several reviews (17, 30–32) and a brief insight and comparison complements the understanding of membrane degradation mechanisms in RFBs. For Nafion<sup>®</sup>, which is

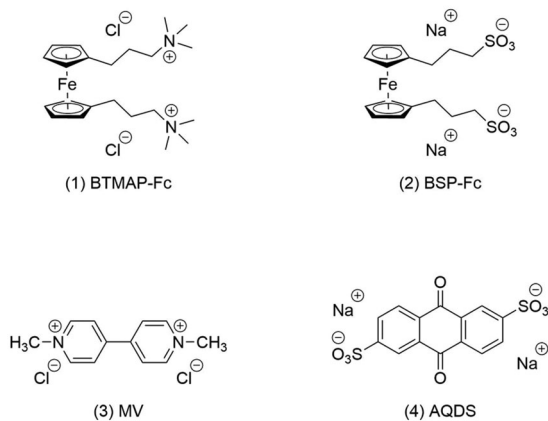
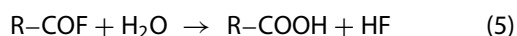
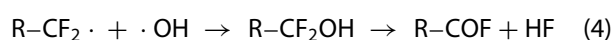


**Figure 3.** Redox mediators used by Gao *et al.* (29).

widely used in proton exchange membrane FCs (PEMFCs), *ex situ* aging tests and investigations are also interesting for RFB applications (17, 33).

In studies conducted by Healy *et al.* on PFSA membranes, their degradation was monitored during FC operation as well as *ex situ* with  $^{19}\text{F}$  NMR and mass spectrometry (MS) (34). They observed similar degradation products for membranes used in FCs and for membranes aged *ex situ* in Fenton's reagent, a mixture of 29% hydrogen peroxide with 4 ppm or 16 ppm of  $\text{Fe}^{2+}$ , at  $88^\circ\text{C}$  for 24 h. From the molecule fragments found, a degradation mechanism which involves the destruction of the perfluorinated polymer backbone by unzipping it step by step was proposed, where terminal carboxylic groups at the backbone are attacked by hydroxyl radicals. The occurring reactions are shown in eq. (3), (4), and (5) (32, 34):



Schulze *et al.* as well as Chen *et al.* examined aged PEMFC Nafion<sup>®</sup> membranes with X-ray photoelectron spectroscopy (XPS) (35, 36). Schulze *et al.* showed that the exposition of Nafion<sup>®</sup> 117 to X-rays for 20 h resulted in a decrease in the binding energy of the C1s signal in the XPS spectra as well as lowered sulfur and oxygen concentrations, indicating the cleavage of C-F bonds and a decomposition of the sulfuric acid-bearing side chains. Ion etching with  $\text{Ar}^+$  ions amplified the observed processes. The membrane was also reported to be brittle after testing (35).

Chen *et al.* did not report any decomposition of Nafion<sup>®</sup> 112 after exposition to X-rays for 2 h (36). However, when exposed to Fenton's reagent (10%wt hydrogen peroxide and up to 300 ppm  $\text{Fe}^{2+}$  at up to  $80^\circ\text{C}$  for up to 24 h), a decrease in the C1s signal in the XPS experiments was found again. Infrared (IR) spectroscopy also showed a decrease in the signal intensity corresponding to the  $\text{CF}_2$  stretching, further providing evidence for membrane degradation. Mechanistically, an attack of hydroxyl and hydroperoxyl radicals on defects in the Nafion<sup>®</sup> backbone (such as C-H and C=C bonds) as well as on the sulfonic acid groups was suggested (36). This is in accordance with the mechanism proposed by Healy *et al.* as well as further studies (34, 37–39). An overview over the Nafion<sup>®</sup> degradation pathways in FCs can be found in Figure 4.

## Hydrocarbon membranes

A membrane material used in early VRFBs is polyethylene (PE), which was tested regarding its suitability by Hwang and Ohya (28). A chlorosulfonated, radiation crosslinked PE membrane with a thickness of  $20\ \mu\text{m}$  was stored for 60d in fully charged electrolyte based on 2M sulfuric acid and 2M vanadyl sulfate. The resistivity of the membrane was measured after 0, 30, and 60 days, and it increased depending on the charging/discharging current applied from  $5.05\text{--}5.70\ \Omega\text{cm}^2$  to  $6.34\text{--}9.67\ \Omega\text{cm}^2$  after 60 days. A non-crosslinked PE membrane was tested as well and showed significant deterioration after the aging test. The crosslinked PE membranes did, however, not show any visible degradation.

An emerging aromatic membrane material for RFBs is sulfonated poly(ether ether ketone) (SPEEK) (Figure 5) as well as composites and derivatives based on it (22, 40–45).

Xi *et al.* synthesized a range of SPEEK membranes with different degrees of sulfonation and casting solvents (44). The membrane stability was assessed with *ex situ* immersion tests in  $0.1\text{M}\ \text{VO}_2^+$  solutions and  $1.5\text{M}\ \text{VO}_2^+$  solutions for 42d. Three SPEEK membranes based on N,N-dimethylformamide (DMF) as casting solvent were tested with sulfonation degrees of 67%, 80%, and 87%, as well as three additional membranes with N,N-dimethylacetamide (DMAc), N-methyl-2-pyrrolidone (NMP), and dimethyl sulfoxide (DMSO) as casting solvent, respectively, at a sulfonation of 67% were evaluated. A general increase in mass loss and emergence of  $\text{VO}^{2+}$  was observed for higher sulfonation degrees, which was ascribed to a stronger water uptake and therewith higher  $\text{VO}_2^+$  concentrations inside the membrane, leading to chemical reactions of the  $\text{VO}_2^+$  with the membrane. Apart from the membrane casted with DMSO, the DMF membranes were the most stable ones during the immersion tests for comparable degrees of sulfonation. During an *in situ* cycling test, however, the cell with the DMSO membrane exhibited a sudden decrease in capacity after 90 cycles, implying that the membrane was prone to degradation under real operation conditions. Therewith the DMF casted membranes were the most stable ones from the tested group of membranes.

In another study, Xi *et al.* tested manufactured SPEEK membranes with 61% sulfonation at different temperatures regarding their performance and aging in VRFBs (27). While the membrane showed an almost temperature-independent Coulombic efficiency (CE) due to low vanadium crossover, it ruptured after around 100 cycles of operation at  $50^\circ\text{C}$ . The authors assumed that

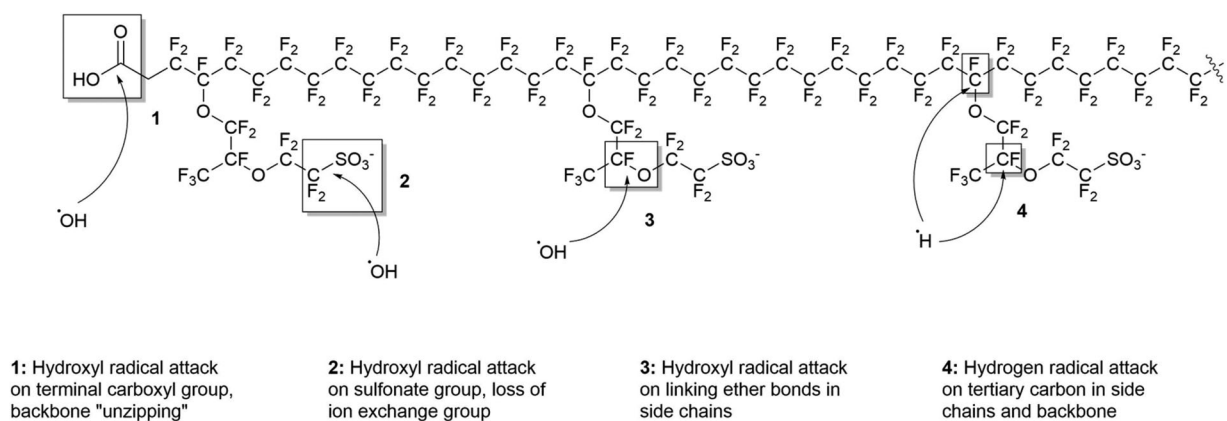


**Figure 4.** Nafion® degradation mechanisms in PEMFCs according to Zatoń *et al.* (17).

the  $\text{VO}_2^+$  oxidized the membrane at elevated temperatures which led to battery failure.

Yuan *et al.* probed the stability of SPEEK membranes *in situ* during cycling experiments in VRFBs as well as *ex situ* with immersion tests (46). Membranes with degrees of sulfonation between 74% and 91% were immersed into 0.15M  $\text{VO}_2^+$  solution for 30d as well as in 1.5M  $\text{VO}_2^+$  solution for 30 h at 40°C each. The concentration of emerging  $\text{VO}^{2+}$  was tracked photometrically for the samples in the 0.15M solution and a correlation between sulfonation and  $\text{VO}^{2+}$  concentration was found. SPEEK samples with a higher degree of sulfonation yielded a higher  $\text{VO}^{2+}$  concentration and therefore degraded faster, implying a degradation mechanism connected to the sulfonic acid groups. Scanning electron microscopy (SEM) imaging showed severe cracks in the samples soaked in 1.5M  $\text{VO}_2^+$  solution for 30 h, with the sample at 91% sulfonation becoming brittle and breaking into pieces.  $^1\text{H}$  NMR and IR spectroscopy of the samples showed no sign of chemical sulfonic acid degradation, however, the polymer backbone is attacked at the ether bonds. Further degradation experiments at varying sulfuric acid concentrations in 0.15M  $\text{VO}_2^+$  showed that the membrane ages faster at higher

acid concentrations, leading to the development of a reaction mechanism in which the protonated backbone was degraded and oxidized by  $\text{VO}_2^+$ . While the sulfonic acid group itself did not get attacked, its electron-drawing properties supports the oxidation of the polymer (Figure 6). For comparison, an *in situ* test was done with the 91% sulfonated SPEEK membrane in a VRFB cell. While the cell reached an EE of 84% at 80 mA/cm<sup>2</sup>, the EE decreased after 100 cycles due to membrane degradation. Examination of the membrane with SEM and  $^1\text{H}$  NMR confirmed the results found in the *ex situ* tests. Additionally, the SEM images showed that the membrane side facing the PHC degraded significantly stronger than the side facing the NHC, suggesting that  $\text{VO}_2^+$  was mainly responsible for the degradation. Therewith could be concluded when applying sulfonic acid containing membranes, a delicate balance has to be found, as a higher sulfonic acid concentration improves ionic conductivity, but decreases stability simultaneously.

Mai *et al.* investigated a SPEEK polymer with a tetramethyldiphenyl structure element (41). Its stability was evaluated in a cycling test over 80 cycles with an electrolyte concentration of 1.5M vanadium and a sulfuric acid concentration of 3M at a current density of 50 mA/cm<sup>2</sup>. While the efficiency of the cell indicated suitable conductivity, the cycling test was too short to decisively assess the long-term stability. Additionally, SEM imaging showed damage at both sides of the membrane and therewith clear signs of degradation.

Apart from VRFBs, SPEEK was also tested as a membrane in ICRFBs by Sun *et al.* (22) They prepared membranes with a degree of sulfonation of 55% which were immersed into a solution of 1M  $\text{Fe}^{2+}$  and 1M  $\text{Cr}^{3+}$  in 3M HCl for 22d. The resulting deviations regarding membrane weight, thickness, and length were monitored. While the weight and length of the membranes

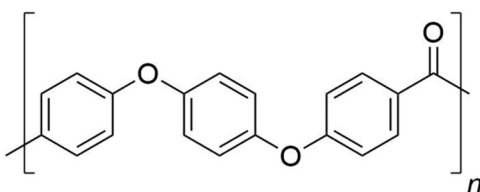


**Figure 5.** Poly(ether ether ketone) used as base for membrane materials. The p-phenylene can be replaced with other aromatic groups like biphenyl or fluorene units. SPEEK is made from the pictured polymer by sulfonation, which leads to a functionalization of arylene rings with sulfonic acid groups up to a certain degree.

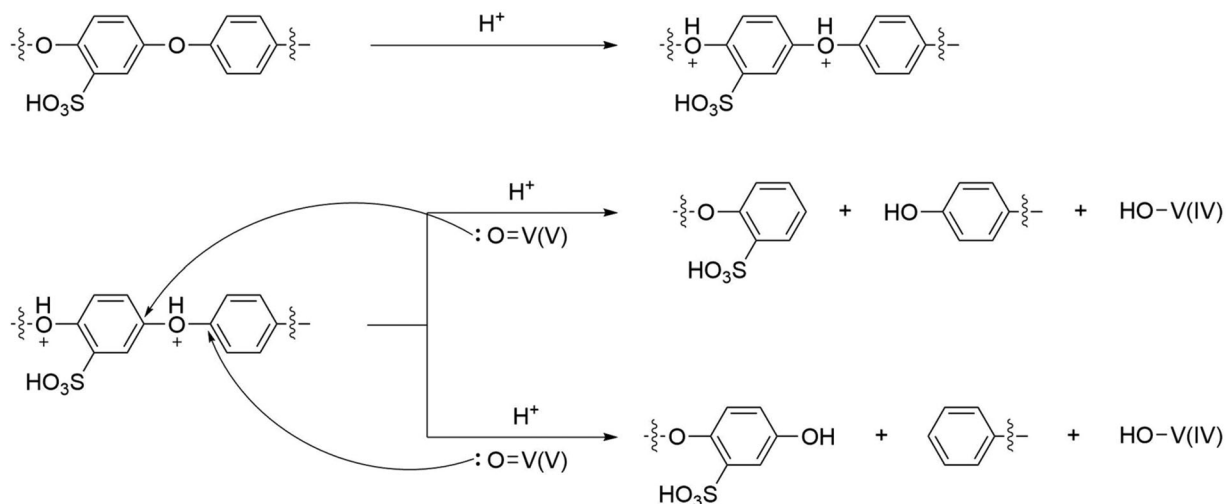


**Figure 6.** Degradation of a SPEEK membrane *via* the attack of  $\text{VO}_2^+$  at the protonated ether bounds in the acidic electrolyte according to Yuan *et al.* (46).

increased and the thickness decreased at first, the membrane dimensions did not change significantly afterwards, indicating good stability of SPEEK in ICRFBs.

In addition to SPEEK, similar sulfonated aromatic polymers with different connecting groups between the *p*-phenylene fragments were tested as RFB membranes. For example, S-Radel® membranes utilize a sulfone group instead of the ketone group as linker in the polymer backbone, yielding sulfonated polyether sulfone (SPES) materials (Figure 7) (47–50).

Chen *et al.* investigated the synthesis and properties of a SPES-based membrane for VRFBs (47). For the stability examination, an oxidative stress test in Fenton's reagent composed of 3%wt  $\text{H}_2\text{O}_2$  and 2 ppm  $\text{FeSO}_4$  at  $80^\circ\text{C}$  was applied. While all membranes tested were dissolved in the solution in under 5 h, the results show clear trends regarding degradation time and degree of sulfonation on one hand as well as functionalization on the other hand. A higher degree of sulfonation led to a larger water uptake and faster degradation.

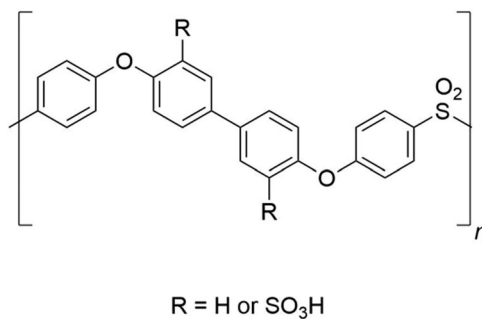


**Figure 7.** S-Radel® membrane reproduced after Chen and Hickner (50). The structure is similar to SPEEK, although the ketone group is replaced by a sulfone group.

Functionalizing the arylene units with methyl groups in *ortho* position relative to the ether linkages yielded membranes of higher oxidative stability and lower water uptake, whereas the IEC was similar compared to non-functionalized membranes.

S-Radel® membranes were tested intensively regarding their chemical stability by Kim *et al.* (48) In a VRFB cycling experiment using electrolyte with a total vanadium concentration of 2M and a total sulfate concentration of 5M, a sudden decrease in CE after 460 h of operation was observed. The used S-Radel® membrane showed severe defects in form of delamination afterwards. Further cycling tests with a reduced total vanadium concentration of 1.7M were done and the membrane was imaged using optical microscopy as well as SEM after 125 h and after 254 h of operation. The membrane did not rupture during this test, however, cracks were observed. After 254 h, delaminated membrane flakes were also visible. The membrane side facing the PHC degraded more severely than the side facing the NHC, whereas the areas covered by the gasket did not show signs of aging. The authors corroborated their results with an *ex situ* aging test, for which the S-Radel® membrane was immersed in 0.1M  $\text{VO}_2^+$  for 170 h at  $22^\circ\text{C}$  and  $40^\circ\text{C}$ , respectively. As a result, the membranes exhibited degradation and a significant increase in  $\text{VO}^{2+}$  concentration was measured by UV/Vis spectroscopy (even more at elevated temperatures), while no  $\text{VO}^{2+}$  was measured in a parallel experiment with a Nafion® 117 membrane. When the S-Radel® membrane was soaked in 1.7M V solution of different oxidation states, the membrane in  $\text{VO}_2^+$  solution showed cracks all over the surface after 80 h, while the samples soaked in  $\text{VO}^{2+}$  solution for 40d and in  $\text{V}^{3+}$  as well as



$\text{VO}^{2+}$  solution for 100 h looked almost pristine. Raman spectroscopy of the membrane showed that the symmetric stretching vibration intensity of the  $\text{SO}_2$  units in the sulfonate groups decreased when the membrane was immersed in  $\text{VO}^{2+}$  or in  $\text{VO}_2^+$  containing electrolyte solution compared to membrane samples soaked in sulfuric acid. The authors assigned this result to ion exchange of the sulfonic acid protons against vanadium ions in the membrane.

Hickner *et al.* investigated the aging of S-Radel® membranes further and suggested a reaction pathway for the  $\text{VO}_2^+$  degradation (50). For this purpose, the membrane was placed in a solution containing 1.7M  $\text{VO}_2^+$  and 3.3M sulfuric acid for 72 h at 40°C. The resulting material was brittle and no longer transparent, but yellowish. IR spectroscopy gave a reduced signal intensity for the sulfonic acid stretching vibration of the degraded membrane, whereas IEC and results of thermogravimetric analysis showed no effect of artificial aging procedure on the membrane, indicating an exchange regarding acidic protons against vanadium ions and interaction with physisorbed water molecules, but no decomposition of the sulfonic acid groups. Additionally, a new signal was identified and assigned to a quinone functionality. XPS results supported the assignment, as an increase in C–O functionalities was observed. Hickner *et al.* therefore proposed a reaction mechanism involving a vanadium(V) oxo peroxy compound as active species, which oxidizes the arylene units to quinones, inducing polymer backbone destruction (Figure 8).

Choi *et al.* synthesized SPES membranes from a sulfonated poly(thioether ether sulfone) (SPTES) precursor by oxidation of the thioether groups (51). Both materials were tested during *in situ* cycling tests in a VRFB cell as well as in *ex situ*  $\text{VO}_2^+$  oxidation experiments. The *ex situ* tests were done in 0.1M  $\text{VO}_2^+$  solution for over 1400 h and in 1.5M  $\text{VO}_2^+$  solution for over 300 h. With UV/Vis monitoring, an increase of  $\text{VO}^{2+}$  was measured over time, but the  $\text{VO}^{2+}$  concentration was significantly lower for the oxidized SPES membranes compared to the thioether-containing SPTES membranes, indicating reduced stability for the latter material. The SPES samples showed almost no  $\text{VO}^{2+}$  emergence in the 0.1M  $\text{VO}_2^+$  solution, while the  $\text{VO}^{2+}$  concentration in the higher concentrated  $\text{VO}_2^+$  solution was determined to be below or around 5 mM and was thus comparable to the  $\text{VO}^{2+}$  concentration determined for the blank sample containing no membrane at all. However, there was still a trend found regarding the degree of sulfonation. Membranes with a higher percentage of sulfonated monomers as educts produced slightly more  $\text{VO}^{2+}$ , respectively degraded stronger. This was even more pronounced for the non-oxidized SPTES material, for which

$\text{VO}^{2+}$  concentrations of up to 20 mM were observed in both aging solutions (although a longer time was necessary to reach a plateau in the lower concentrated  $\text{VO}_2^+$  solution). For the *in situ* aging experiments, the SPES and the SPTES membrane were used for 400 charge/discharge cycles in a VRFB. The cell with the SPTES membrane showed irregular behavior after 150 cycles, indicating a damaged membrane, which corroborates the findings from the *ex situ* degradation experiments. The SPES membrane, however, yielded a permanently high CE and only a slight decrease in energy efficiency over the complete runtime as well as better capacity retention than Nafion® 115. After the cycling test, the membranes were investigated with  $^1\text{H}$  NMR and new signals were found for the SPTES material, which indicated the formation of thiols and sulfoxides and therefore polymer backbone degradation at the electron-rich thioether groups. The SPES membrane showed additional peaks as well, albeit with a distinctly smaller signal intensity, which could be assigned to phenolic protons. This means that the SPES membrane was fragmented at the ether linkages, although less intensely as the SPTES membrane. The authors noted that the *in situ* cycling test depicts membrane degradation induced by electrochemical aging in addition to the chemical aging due to the  $\text{VO}_2^+$  species and is therefore more severe than expected from the *ex situ* tests. Additionally, they suggest that the electron-withdrawing effect caused by the sulfone groups stabilizes the membrane against oxidative degradation by  $\text{VO}_2^+$  species (Figure 9).

### Anion-exchange membranes

AEMs promote the diffusion of negatively charged species, but retain cations by employing positively charged ionic functionalities such as quaternary ammonium, imidazolium, pyridinium, or sulfonium groups. In RFBs relying on the oxidation and reduction of metal ions such as vanadium, iron, or chromium, this has the advantage that the crossover of the redox-active species is less likely, however, most anions diffuse slower through the membrane compared to protons through CEMs (52).

Mohammadi and Skyllas-Kazacos evaluated Selemion® AMV (Asahi Glass Co.) as membrane for VRFBs (26). (The Selemion® trademark is available as CEM or AEM, which can lead to misunderstandings.) In an *ex situ* immersion test, the AMV membrane lost between 6% and 7% of its weight in 0.1M  $\text{VO}_2^+$  solution after two months. This result was confirmed by UV/Vis spectroscopy of the emerged  $\text{VO}^{2+}$ . Another investigation of Selemion® AMV (among other membranes) was

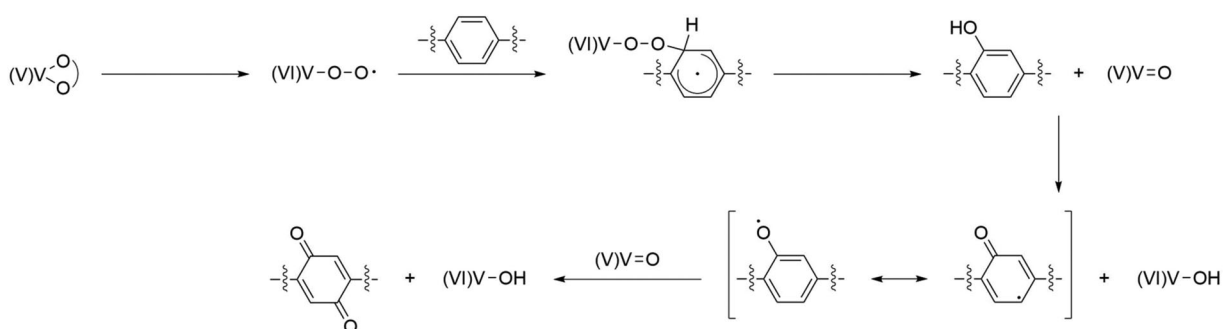


**Figure 8.** S-Radel® degradation mechanism according to Chen and Hickner involving V(V) oxo peroxy species (50).

done by Xi *et al.* (27) However, because of its high voltage overpotential and therefore low VE as a result of the membrane's high resistivity, Selemion® AMV was omitted from the prolonged cycling test at different temperatures conducted by the authors.

Xing *et al.* functionalized a poly(ether ether sulfone) (PEES) cation exchange material with three different positively charged ionic groups to implement them as AEMs for VRFBs (53). The charge-bearing groups were protonated tertiary amines (PSf-PTA-1.4), protonated tertiary amines separated from the polymer backbone via spacer molecules (PSf-c-PTA-1.4) and quaternary amines with the same spacer (PSf-c-QA-1.2), as shown in Figure 10. The membrane materials were evaluated in an *ex situ* degradation test by immersing the membranes in solutions of 0.15M  $\text{VO}_2^+$  as well as 1.5M  $\text{VO}_2^+$  in 3M sulfuric acid at 40°C for 720 h. From the lower concentrated samples, the  $\text{VO}^{2+}$  concentration was measured regularly with UV/Vis spectroscopy. The most  $\text{VO}^{2+}$  emerged from the test with PSf-PTA-1.4, while from both membranes with spacer molecules, the one with PSf-c-QA-1.2 yielded a slightly higher  $\text{VO}^{2+}$  concentration compared to the membranes with PSf-c-PTA-1.4. From the non-functionalized PEES, almost no  $\text{VO}^{2+}$  emerged. The membrane samples, which were stored in the higher concentrated  $\text{VO}_2^+$  solution were withdrawn after 720 h and  $^1\text{H}$  as well as  $^{13}\text{C}$  NMR was measured. While for PSf-PTA-1.4, the protonated tertiary amine group as well as the polymer backbone ether bond were attacked, for PSf-c-PTA-1.4, the protonated tertiary amine was dealkylated, but the backbone was not severed. For PSf-c-QA-1.2, no degradation products were found with NMR. In an *in situ* VRFB test at 120 mA/cm<sup>2</sup>, however, PSf-c-QA-1.2 suffered from the highest capacity loss (comparable to Nafion 115) and after 25d (or approximately 700 cycles), the EE dropped rapidly, indicating a damaged membrane. The PSf-c-PTA-1.4 membrane showed the highest EE and good capacity retention, but it also exhibited a large drop in its EE after 30d (or approximately 850 cycles).

PSf-PTA-1.4 had the highest capacity retention, the lowest EE, but was actually the most stable material in the *in situ* test, only showing an EE drop after 36d (or approximately 1050 cycles). This illustrates that the *ex situ* tests cannot always predict the *in situ* performance. The authors claimed that the *in situ* degradation stems from mechanical strain due to deposition of the active vanadium species at the membrane and the following dissolution.

Yuan *et al.* studied the aging of another PEES membrane material (54). They crosslinked a chloromethylated PEES with 0.4 mmol (CMPSF-0.4), 0.8 mmol (CMPSF-0.8), and 1.0 mmol (CMPSF-1.0) of 4,4'-bipyridine, forming positively charged bipyridinium cations. The resulting materials were tested as membrane materials for VRFBs by an immersion test in 0.15M  $\text{VO}_2^+$ /3M sulfuric acid at 40°C for 500 h. The spectroscopically measured  $\text{VO}^{2+}$  concentration correlated with the bipyridinium content; a higher amount of crosslinker led to a faster degradation. No reference material was tested, but since Xi *et al.* used the same degradation conditions for their *ex situ* degradation tests, numbers can be compared. The non-crosslinked PEES membranes from Xi *et al.* showed 20-45 mM of  $\text{VO}^{2+}$  concentration after 500 h, (53) whereas the measured concentrations of the crosslinked membranes from Yuan *et al.* only yielded between 2.5 and 7 mM of  $\text{VO}^{2+}$  after 500 h (54). This means that the crosslinking seems to be generally favorable for the oxidative stability of PEES-based AEMs. In an accelerated aging test, the CMPSF-1.0 were soaked in a  $\text{VO}_2^+$  solution with a concentration of 1.5M (but otherwise the same conditions as before) for 18d. Membrane samples were retrieved after 3d, 7d, and 12d to compare their performances when assembled into a VRFB stack with the pristine CMPSF-1.0 membrane. No significant drop in cell efficiencies was noted, however, after 18d in the *ex situ* aging solution, the membrane became reddish (due to the incorporation of  $\text{VO}_2^+$ , which could be reverted by soaking in sulfuric acid) and brittle. SEM imaging also showed that

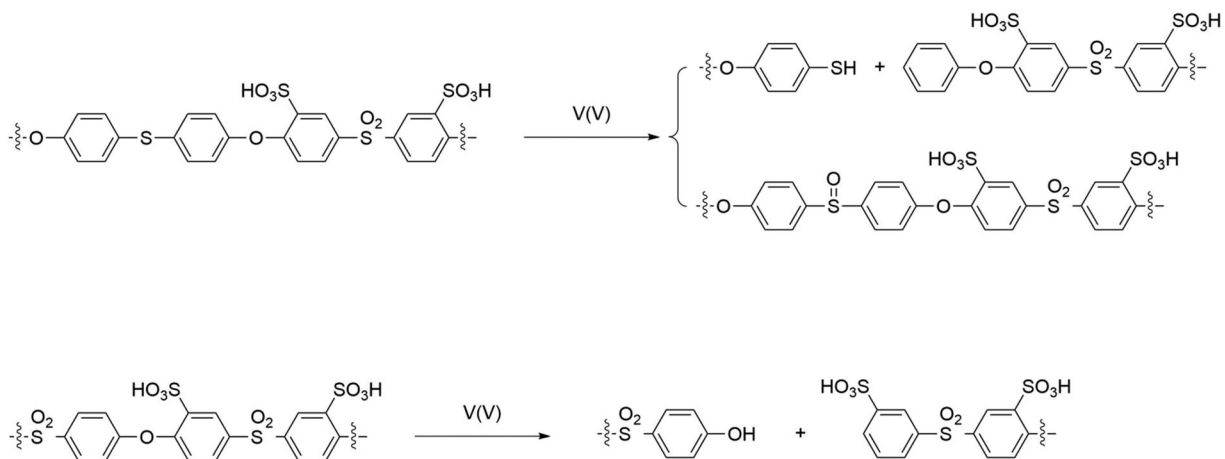


**Figure 9.** SPTES and SPES degradation mechanisms according to Choi *et al.* (51).

the membrane was severely damaged. IR and Raman spectroscopy revealed the emergence of phenolic hydroxyl groups as well as newly formed vanadium oxygen bonds in the degraded membranes and ruled out the presence of bipyridine monomers. The authors therefore suggested a degradation mechanism, where

the ionic bipyridinium groups are stable, but induce a nucleophilic attack of  $\text{VO}_2^+$  oxygen on the ether bonds of the polymer backbone due to their electron-withdrawing properties. The resulting polymer fragments contain the phenolic groups and the newly formed vanadium oxygen species (Figure 11).

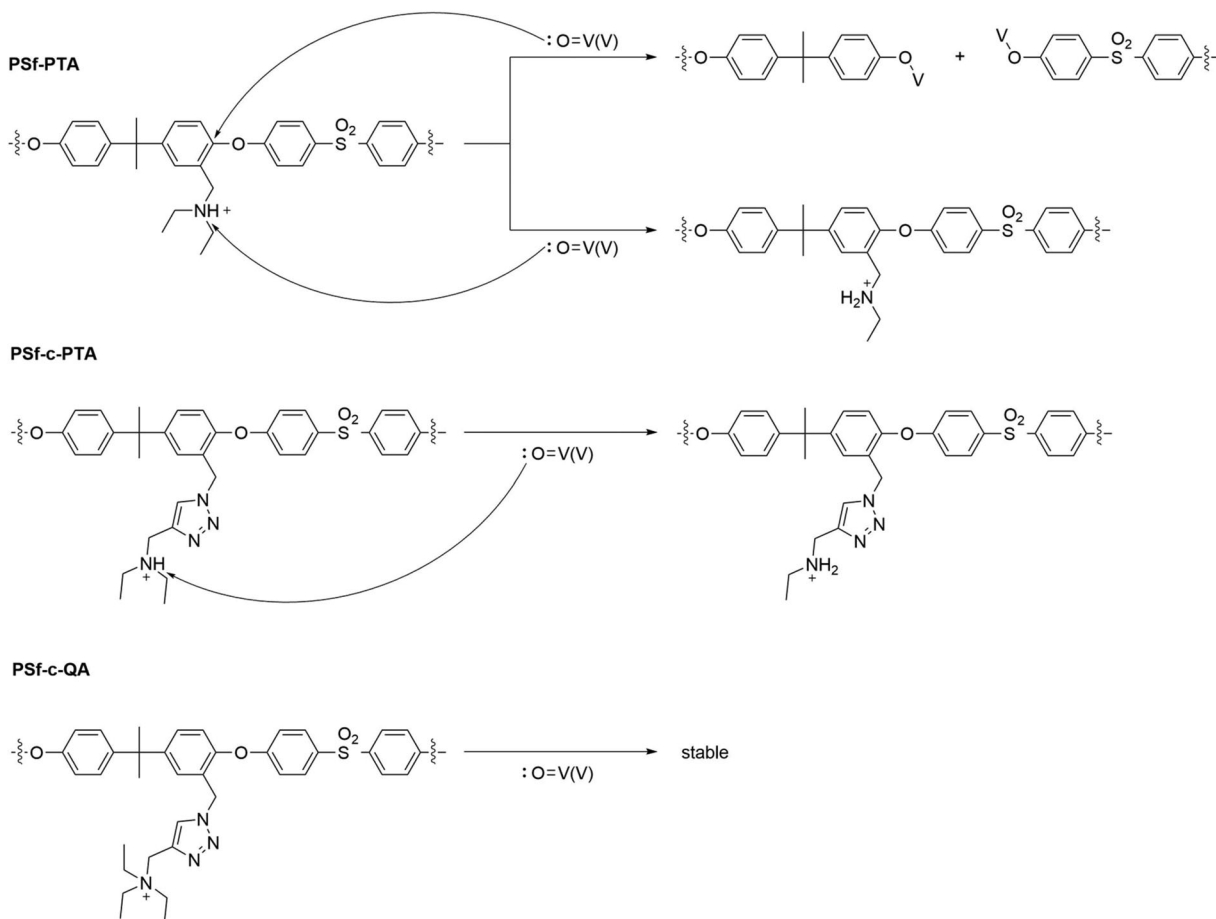


**Figure 10.** Mechanisms of SPES AEM degradation according to Xing *et al.* (53).

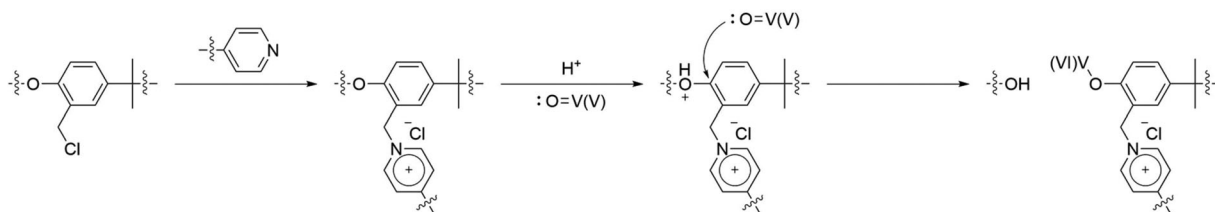


**Figure 11.** Degradation mechanism of bipyridine-crosslinked PEES material from the studies of Yuan *et al.* (54).

Further studies on the degradation of the PEES polymer based membranes, but with different cationic groups was conducted by Jung *et al.* (55) PEES was functionalized with trimethyl ammonium methylene groups and immersed into  $3\text{M VO}_2^+$  in  $3\text{M}$  sulfuric acid at  $30^\circ\text{C}$ . While ion conductivity and IEC decreased over a range of 30d, the membrane was too brittle after 90d for further analysis.

An investigation of aged Fumatech® fap-450 AEMs utilized in commercial VRFBs was conducted by Herrmann *et al.* (52) Six membranes from three stacks were chosen as samples; one stack was operated for three years (membrane samples from first cell and middle cell), one stack was operated for one year at higher SOC (membrane samples from middle cell and last cell), and one stack was contaminated with silicone oil (membrane samples from first cell and middle cell). In cycling tests at current densities between  $25$  and  $100\text{ mA/cm}^2$ , the samples out of the 3 years operated stack exhibited the highest CE, although the sample from first cell caused a large drop in efficiency at the highest current density, *i.e.*  $100\text{ mA/cm}^2$ . For the membranes contaminated with silicon oil, the second-highest CEs were measured, which also were in the range of the pristine membrane. The membranes out of the stack operated at high SOC showed significantly lower CEs, especially the membrane which was employed in the middle cell of the stack. Concerning the VEs, all membranes performed at slightly lower efficiencies compared to the pristine membrane. Proton diffusivity measurements showed that the diffusivities of the 3 year membranes were lower than for the pristine material, while all other samples showed an increased diffusivity. The authors attribute this to blocking and state this as the reason for the sudden decrease of the CE during battery testing with the sample from the first cell of the 3 year old stack. These results show that within one stack, different severities and types of degradation can occur. For the sample from the middle cell of the 1 year old stack, a reduced IEC and swelling ratio was noticed, making the loss of ion-exchange groups the reason for its lowered CE and VE. Concludingly, the authors suggest that the

membrane pores might be blocked after long operation times, but operating a stack at high SOC induced also degradation of the membrane material itself, which was confirmed by small angle X-ray scattering and differential scanning calorimetry, yielding a significant change in crystallinity compared to pristine membranes. The contamination with silicone oil did not deteriorate the membrane.

### Non-ionic separators

Membranes, which do not utilize ionic groups, but use their pore size to exclude certain species from passing through it, are called non-ionic or microporous separators.

Daramic®, a PE-based separator regularly applied as lead acid battery separator, was tested as a RFB membrane in a vanadium-based electrolyte by Mohammadi and Skyllas-Kazacos (26). The membrane sample was immersed in  $0.1\text{M VO}_2^+$  solution for 60d and a mass loss of 23% and a reduction of  $\text{VO}_2^+$  to  $\text{VO}^{2+}$  of 16% (for a  $0.30\text{ g}$  sample) and 33% (for a  $0.62\text{ g}$  sample) occurred. Since the separator also exhibited low selectivity, pristine Daramic® was not investigated further in this study.

### Amphoteric and composite membranes

Composite membranes consist of different materials with various properties. When CEM and AEM materials are combined in one membrane, bipolar amphoteric membranes are obtained to compensate the drawbacks and utilize the advantages of both materials.

In addition to pristine Daramic®, Mohammadi and Skyllas-Kazacos modified the material with divinylbenzene (DVB) by polymerizing DVB soaked into the membrane to obtain composite Daramic® and sulfonated the resulting material to yield sulfonated composite Daramic® (26). After soaking the membranes in  $0.1\text{M VO}_2^+$  for 60d, a mass loss of 10% for the composite Daramic® and 17-18% for the sulfonated composite Daramic® was noted. Although the amount of  $\text{VO}_2^+$  reduced to  $\text{VO}^{2+}$  was slightly lower for both materials

compared to pristine Daramic<sup>®</sup>, it was not as low as one could expect from the diminished mass loss. In a follow-up experiment, the membranes were aged in a 2M VO<sub>2</sub><sup>+</sup> solution for 180d and resistivity as well as permeability of VO<sub>2</sub><sup>+</sup> were monitored. For all samples, the resistivity decreased and the permeability increased over time. Sulfonation led to a generally lower resistivity, while the VO<sub>2</sub><sup>+</sup> permeation changed ambiguously. A longer DVB crosslinking duration increased the resistivity significantly, while permeability decreased. The authors suggest that this is due to a thicker DVB layer on the membranes which protects the PE backbone from oxidation. This is also visible in SEM images of the Daramic<sup>®</sup> materials, where the DVB can be seen in the pores of the aged membrane, whereas the non-functionalized aged material clearly shows enlarged pores. Additionally, the IEC of the sulfonated composite Daramic<sup>®</sup> membrane was examined before and after aging for 180d in 2M VO<sub>2</sub><sup>+</sup>, showing a 23% (for 1 h of crosslinking) and a 25% (for 3 h of crosslinking) decrease, respectively, although the initial IEC of the latter sample was slightly higher. In an *in situ* aging experiment conducted in a VRFB running for 180d with the sulfonated composite Daramic<sup>®</sup>, resistivity and VO<sub>2</sub><sup>+</sup> permeability was monitored once again, yielding similar results compared with the *ex situ* test mentioned above, however, the decrease in resistivity and the increase in permeability was not as large as in the *ex situ* experiment.

A composite membrane based on a sulfonated polyimide and the biopolymer chitosan was investigated by Yue *et al.* (56) The chitosan strands were used to crosslink the sulfonated polyimide by ionic interaction between sulfonic acid groups and protonated amine groups of the chitosan. A degradation experiment for which composite membranes with chitosan infiltration times of 6, 12, 24, and 36 h were used was conducted in a 0.5M VO<sub>2</sub><sup>+</sup> solution in 2M sulfuric acid for 20 days. Afterwards, mass losses of 5.56% to 6.12% were observed. The composite membrane with a chitosan infiltration time of 24 h showed the lowest mass loss, however, it was still more than two times higher compared to the reference, Nafion<sup>®</sup> 117.

Donten *et al.* prepared composite membranes for VRFB applications based on a heavily crosslinked supporting polymer and embedded poly(vinyl pyrrolidone) (PVP) on a porous poly(vinyl chloride) silica substrate (57). The PVP becomes protonated in acidic media, making the composite an AEM. Membranes with PVP contents between 6% and 16% were fabricated, since higher concentrations led to dissolution of the PVP coating and lower concentrations did not make the casting solution viscous enough. For durability tests, the membrane was stored in 1.6M VO<sub>2</sub><sup>+</sup>/2M sulfuric

acid for 1000 h and the VO<sub>2</sub><sup>+</sup> concentration was measured using UV/Vis spectroscopy. For both tested samples (8% and 14% PVP), an increase in VO<sub>2</sub><sup>+</sup> concentration was measured, while no VO<sub>2</sub><sup>+</sup> was found in reference samples containing the silica substrate or nothing at all. In a second test lasting for 24 h, the polymer matrix and the PVP were investigated separately. This showed that mainly the polymer matrix degraded while PVP was not as prone to oxidation, suggesting a change or modification of matrix materials could improve the overall membrane stability.

## Conclusion

A wide range of membrane materials, characterized regarding their chemical and mechanical stability, was summarized and compared in this review. While *ex situ* accelerated aging in RFB electrolyte of various concentrations was the predominant method of examination applied in literature, some studies also included long-term *in situ* membrane aging during battery operation. Interestingly, the results of *in situ* battery cell tests do not always yield similar results compared to the *ex situ* aging experiments. This is due to the higher complexity of the real battery setup, where the membrane is additionally strained mechanically, through electrolyte convection, and because of ion migration. Hence, membranes tested in battery setups are more likely affected by blockage, while membranes in *ex situ* setups exhibit a decrease in resistivity more often due to pore widening. Nonetheless, the *ex situ* accelerated aging tests are an important tool to assess the long-term chemical stability of the membrane materials when exposed to electrolyte. The demand for real world commercial application is a material which is (next to a cheap price and good selectivity) stable for years to decades. Such extended timespans can be not realistically investigated by *in situ* tests.

Degradation pathways of the membrane reported in literature can mainly be separated into two classes: oxidative decomposition and pore blocking. Pore blocking results in a lowered membrane permeability and increased resistivity. The blocking species are mostly the redox active compounds such as vanadium in VRFBs or electrolyte contaminants. Regarding oxidative decomposition, either the membrane backbone can be attacked, which results in breakdown of the material and yields membrane fragments, or the functional groups responsible for the ion exchange can be affected. This can result in pore widening and/or a loss of ion exchange capabilities.

Recently, several promising novel membrane materials have been developed. Especially SPEEK and

its derivatives receive a lot of attention because of their cheap price and good selectivity. However, regarding (especially chemical) stability, which is the main focus of this review, perfluorinated membranes like Nafion® are still the benchmark.

## Outlook

Because of the commitment towards renewable energy sources and the associated need for electrical energy storage systems it is assumed that the demand for RFBs will increase further. With this, interest in component and especially membrane stability will rise as well.

Next to the well-researched classical inorganic RFBs, nonaqueous RFBs based on organic electrolytes and/or organic redox-active species are gaining importance because of possibly higher cell potentials, wider temperature ranges, and high energy densities (58–60). These systems, however, have to be regarded separately in terms of membrane development, since organic electrolytes lead to considerable swelling of most polymer based membranes, which makes inorganic porous ceramics the favored separator in this case (61–63).

A trend which is clearly visible is the research on composite membranes. While there is only a limited number on long-time degradation studies on composite membrane materials, they show a great potential in increasing membrane stability and selectivity by using different materials with different properties (e.g. coating of a very selective material with a stable shielding material). This opens up new possibilities for inorganic and organic RFBs alike.

## Acknowledgements

The authors thank Pavel Mardilovich and Enerox GmbH for helpful discussions and comments. Financial support from the FFG run framework of COMET – Competence Centers for Excellent Technologies by BMVIT, BMDW as well as the Province of Lower Austria and Upper Austria is gratefully acknowledged. The authors acknowledge TU Wien Bibliothek for financial support through its Open Access Funding Program

## Disclosure statement

No potential conflict of interest was reported by the author(s).

## Funding

This work was supported by Austrian Research Promotion Agency – FFG.

## ORCID

Christian M. Pichler  <http://orcid.org/0000-0001-7686-7215>

## References

- [1] Gallo, A.B.; Simões-Moreira, J.R.; Costa, H.K.M.; Santos, M.M.; Moutinho dos Santos, E. Energy Storage in the Energy Transition Context: A Technology Review. *Renew. Sustainable Energy Rev.* **2016**, *65*, 800–822. doi:10.1016/j.rser.2016.07.028.
- [2] Chen, C.; Xue, B.; Cai, G.; Thomas, H.; Stückrad, S. Comparing the Energy Transitions in Germany and China: Synergies and Recommendations. *Energy Rep.* **2019**, *5*, 1249–1260. doi:10.1016/j.egy.2019.08.087.
- [3] Weber, A.Z.; Mench, M.M.; Meyers, J.P.; Ross, P.N.; Gostick, J.T.; Liu, Q. Redox Flow Batteries: A Review. *J. Appl. Electrochem.* **2011**, *41* (10), 1137–1164. doi:10.1007/s10800-011-0348-2.
- [4] Lourenssen, K.; Williams, J.; Ahmadpour, F.; Clemmer, R.; Tasnim, S. Vanadium Redox Flow Batteries: A Comprehensive Review. *J. Energy Storage* **2019**, *25*, 100844. doi:10.1016/j.est.2019.100844.
- [5] Sun, C.; Zhang, H. Review of the Development of First-Generation Redox Flow Batteries: Iron-Chromium System. *ChemSusChem.* **2022**, *15* (1). doi:10.1002/cssc.202101798.
- [6] Skyllas-Kazacos, M.; Rychcik, M.; Robins, R.G.; Fane, A.G.; Green, M.A. New All-Vanadium Redox Flow Cell. *J. Electrochem. Soc.* **1986**, *133* (5), 1057–1058. doi:10.1149/1.2108706.
- [7] Knehr, K.W.; Kumbur, E.C. Open Circuit Voltage of Vanadium Redox Flow Batteries: Discrepancy Between Models and Experiments. *Electrochem. Commun.* **2011**, *13* (4), 342–345. doi:10.1016/j.jelecom.2011.01.020.
- [8] Agar, E.; Benjamin, A.; Dennison, C.R.; Chen, D.; Hickner, M.A.; Kumbur, E.C. Reducing Capacity Fade in Vanadium Redox Flow Batteries by Altering Charging and Discharging Currents. *J. Power Sources* **2014**, *246*, 767–774. doi:10.1016/j.jpowsour.2013.08.023.
- [9] Pugach, M.; Kondratenko, M.; Briola, S.; Bisch, A. Zero Dimensional Dynamic Model of Vanadium Redox Flow Battery Cell Incorporating All Modes of Vanadium Ions Crossover. *Appl. Energy* **2018**, *226*, 560–569. doi:10.1016/j.apenergy.2018.05.124.
- [10] Nourani, M.; Dennison, C.R.; Jin, X.; Liu, F.; Agar, E. Elucidating Effects of Faradaic Imbalance on Vanadium Redox Flow Battery Performance: Experimental Characterization. *J. Electrochem. Soc.* **2019**, *166* (15), A3844–A3851. doi:10.1149/2.0851915jes.
- [11] Haisch, T.; Ji, H.; Holtz, L.; Struckmann, T.; Weidlich, C. Half-Cell State of Charge Monitoring for Determination of Crossover in VRFB – Considerations and Results Concerning Crossover Direction and Amount. *Membranes.* **2021**, *11* (4), 232. doi:10.3390/membranes11040232.
- [12] Thaller, L.H. Electrically Rechargeable REDOX Flow Cell. US3996064A, 1975.
- [13] Remick, R.J.; Ang, P.G. Electrically Rechargeable Anionically Active Reduction-Oxidation Electrical Storage-Supply System. US4485154, November 27, 1984.

- [14] Zhang, S.; Guo, W.; Yang, F.; Zheng, P.; Qiao, R.; Li, Z. Recent Progress in Polysulfide Redox-Flow Batteries. *Batteries Supercaps* **2019**, *2* (7), 627–637. doi:10.1002/batt.201900056.
- [15] Schwenzer, B.; Zhang, J.; Kim, S.; Li, L.; Liu, J.; Yang, Z. Membrane Development for Vanadium Redox Flow Batteries. *ChemSusChem* **2011**, *4* (10), 1388–1406. doi:10.1002/cssc.201100068.
- [16] Prifti, H.; Parasuraman, A.; Winardi, S.; Lim, T.M.; Skyllas-Kazacos, M. Membranes for Redox Flow Battery Applications. *Membranes* **2012**, *2* (2), 275–306. doi:10.3390/membranes2020275.
- [17] Zatoń, M.; Rozière, J.; Jones, D.J. Current Understanding of Chemical Degradation Mechanisms of Perfluorosulfonic Acid Membranes and Their Mitigation Strategies: A Review. *Sustainable Energy Fuels* **2017**, *1* (3), 409–438. doi:10.1039/C7SE00038C.
- [18] Yuan, X.; Song, C.; Platt, A.; Zhao, N.; Wang, H.; Li, H.; Fatih, K.; Jang, D. A Review of All-Vanadium Redox Flow Battery Durability: Degradation Mechanisms and Mitigation Strategies. *Int. J. Energy Res.* **2019**, er.4607. doi:10.1002/er.4607.
- [19] Vijayakumar, M.; Bhuvanewari, M.S.; Nachimuthu, P.; Schwenzer, B.; Kim, S.; Yang, Z.; Liu, J.; Graff, G.L.; Thevuthasan, S.; Hu, J. Spectroscopic Investigations of the Fouling Process on Nafion Membranes in Vanadium Redox Flow Batteries. *J. Membr. Sci.* **2011**, *366* (1–2), 325–334. doi:10.1016/j.memsci.2010.10.018.
- [20] Luo, Q.; Li, L.; Wang, W.; Nie, Z.; Wei, X.; Li, B.; Chen, B.; Yang, Z.; Sprenkle, V. Capacity Decay and Remediation of Nafion-Based All-Vanadium Redox Flow Batteries. *ChemSusChem* **2013**, *6* (2), 268–274. doi:10.1002/cssc.201200730.
- [21] Jiang, B.; Wu, L.; Yu, L.; Qiu, X.; Xi, J. A Comparative Study of Nafion Series Membranes for Vanadium Redox Flow Batteries. *J. Membr. Sci.* **2016**, *510*, 18–26. doi:10.1016/j.memsci.2016.03.007.
- [22] Sun, C.-Y.; Zhang, H.; Luo, X.-D.; Chen, N. A Comparative Study of Nafion and Sulfonated Poly(Ether Ether Ketone) Membrane Performance for Iron-Chromium Redox Flow Battery. *Ionics* **2019**, *25* (9), 4219–4229. doi:10.1007/s11581-019-02971-0.
- [23] Lemmermann, T.; Becker, M.; Stehle, M.; Drache, M.; Beuermann, S.; Bogar, M.S.; Gohs, U.; Fittschen, U.E.A.; Turek, T.; Kunz, U. In Situ and in Operando Detection of Redox Reactions with Integrated Potential Probes during Vanadium Transport in Ion Exchange Membranes. *J. Power Sources* **2022**, *533*, 231343. doi:10.1016/j.jpowsour.2022.231343.
- [24] Sukkar, T.; Skyllas-Kazacos, M. Membrane Stability Studies for Vanadium Redox Cell Applications. *J. Appl. Electrochem.* **2004**, *34* (2), 137–145. doi:10.1023/B:JACH.0000009931.83368.dc.
- [25] Barbir, F. Main Cell Components, Material Properties, and Processes. In *PEM Fuel Cells*; Barbir, F., Ed.; Elsevier: Amsterdam, **2013**; pp 73–117.
- [26] Mohammadi, T.; Kazacos, M.S. Evaluation of the Chemical Stability of Some Membranes in Vanadium Solution. *J. Appl. Electrochem.* **1997**, *27* (2), 153–160. doi:10.1023/A:1018495722379.
- [27] Xi, J.; Jiang, B.; Yu, L.; Liu, L. Membrane Evaluation for Vanadium Flow Batteries in a Temperature Range of –20–50 °C. *J. Membr. Sci.* **2017**, *522*, 45–55. doi:10.1016/j.memsci.2016.09.012.
- [28] Hwang, G.-J.; Ohya, H. Preparation of Cation Exchange Membrane as a Separator for the All-Vanadium Redox Flow Battery. *J. Membr. Sci.* **1996**, *120* (1), 55–67. doi:10.1016/0376-7388(96)00135-4.
- [29] Gao, M.; Salla, M.; Zhang, F.; Zhi, Y.; Wang, Q. Membrane Fouling in Aqueous Redox Flow Batteries. *J. Power Sources* **2022**, *527*, 231180. doi:10.1016/j.jpowsour.2022.231180.
- [30] Wu, J.; Yuan, X.Z.; Martin, J.J.; Wang, H.; Zhang, J.; Shen, J.; Wu, S.; Merida, W. A Review of PEM Fuel Cell Durability: Degradation Mechanisms and Mitigation Strategies. *J. Power Sources* **2008**, *184* (1), 104–119. doi:10.1016/j.jpowsour.2008.06.006.
- [31] Gubler, L.; Dockheer, S.M.; Koppenol, W.H. Radical (HO<sub>2</sub>·, H<sub>2</sub>O<sub>2</sub> and HOO·) Formation and Ionomer Degradation in Polymer Electrolyte Fuel Cells. *J. Electrochem. Soc.* **2011**, *158* (7), B755–B769. doi:10.1149/1.3581040.
- [32] Ishimoto, T.; Koyama, M. A Review of Molecular-Level Mechanism of Membrane Degradation in the Polymer Electrolyte Fuel Cell. *Membranes* **2012**, *2* (3), 395–414. doi:10.3390/membranes2030395.
- [33] Zhu, L.-Y.; Li, Y.-C.; Liu, J.; He, J.; Wang, L.-Y.; Lei, J.-D. Recent Developments in High-Performance Nafion Membranes for Hydrogen Fuel Cells Applications. *Pet. Sci.* **2022**, *19* (3), 1371–1381. doi:10.1016/j.petsci.2021.11.004.
- [34] Healy, J.; Hayden, C.; Xie, T.; Olson, K.; Waldo, R.; Brundage, M.; Gasteiger, H.; Abbott, J. Aspects of the Chemical Degradation of PFSA Ionomers Used in PEM Fuel Cells. *Fuel Cells* **2005**, *5* (2), 302–308. doi:10.1002/fuce.200400050.
- [35] Schulze, M.; Lorenz, M.; Wagner, N.; Gülzow, E. XPS Analysis of the Degradation of Nafion. *Fresenius' J. Anal. Chem.* **1999**, *365* (1–3), 106–113. doi:10.1007/s002160051454.
- [36] Chen, C.; Levitin, G.; Hess, D.W.; Fuller, T.F. XPS Investigation of Nafion® Membrane Degradation. *J. Power Sources* **2007**, *169* (2), 288–295. doi:10.1016/j.jpowsour.2007.03.037.
- [37] Kundu, S.; Simon, L.C.; Fowler, M.W. Comparison of two Accelerated Nafion™ Degradation Experiments. *Polym. Degrad. Stab.* **2008**, *93* (1), 214–224. doi:10.1016/j.polyimdegradstab.2007.10.001.
- [38] Cipollini, N.E. Chemical Aspects of Membrane Degradation. *ECS Trans.* **2007**, *11* (1), 1071–1082. doi:10.1149/1.2781020.
- [39] Ghassemzadeh, L.; Kreuer, K.-D.; Maier, J.; Müller, K. Chemical Degradation of Nafion Membranes Under Mimic Fuel Cell Conditions as Investigated by Solid-State NMR Spectroscopy. *J. Phys. Chem. C* **2010**, *114* (34), 14635–14645. doi:10.1021/jp102533v.
- [40] Muthulakshmi, R.; Meierhaack, J.; Schlenstedt, K.; Vogel, C.; Choudhary, V.; Varma, I. Sulphonated Poly(Ether Ether Ketone) Copolymers: Synthesis, Characterisation and Membrane Properties. *J. Membr. Sci.* **2005**, *261* (1–2), 27–35. doi:10.1016/j.memsci.2005.03.007.
- [41] Mai, Z.; Zhang, H.; Li, X.; Bi, C.; Dai, H. Sulfonated Poly(Tetramethyldiphenyl Ether Ether Ketone) Membranes for Vanadium Redox Flow Battery Application. *J. Power Sources* **2011**, *196* (1), 482–487. doi:10.1016/j.jpowsour.2010.07.028.

- [42] Li, Z.; Xi, J.; Zhou, H.; Liu, L.; Wu, Z.; Qiu, X.; Chen, L. Preparation and Characterization of Sulfonated Poly(Ether Ether Ketone)/Poly(Vinylidene Fluoride) Blend Membrane for Vanadium Redox Flow Battery Application. *J. Power Sources* **2013**, *237*, 132–140. doi:10.1016/j.jpowsour.2013.03.016.
- [43] Hyeon, D.H.; Chun, J.H.; Lee, C.H.; Jung, H.C.; Kim, S.H. Composite Membranes Based on Sulfonated Poly(Ether Ether Ketone) and SiO<sub>2</sub> for a Vanadium Redox Flow Battery. *Korean J. Chem. Eng.* **2015**, *32* (8), 1554–1563. doi:10.1007/s11814-014-0358-y.
- [44] Xi, J.; Li, Z.; Yu, L.; Yin, B.; Wang, L.; Liu, L.; Qiu, X.; Chen, L. Effect of Degree of Sulfonation and Casting Solvent on Sulfonated Poly(Ether Ether Ketone) Membrane for Vanadium Redox Flow Battery. *J. Power Sources* **2015**, *285*, 195–204. doi:10.1016/j.jpowsour.2015.03.104.
- [45] Chang, S.; Ye, J.; Zhou, W.; Wu, C.; Ding, M.; Long, Y.; Cheng, Y.; Jia, C. A Low-Cost SPEEK-K Type Membrane for Neutral Aqueous Zinc-Iron Redox Flow Battery. *Surf. Coat. Technol.* **2019**, *358*, 190–194. doi:10.1016/j.surfcoat.2018.11.028.
- [46] Yuan, Z.; Li, X.; Hu, J.; Xu, W.; Cao, J.; Zhang, H. Degradation Mechanism of Sulfonated Poly(Ether Ether Ketone) (SPEEK) Ion Exchange Membranes Under Vanadium Flow Battery Medium. *Phys. Chem. Chem. Phys.* **2014**, *16* (37), 19841–19847. doi:10.1039/C4CP03329A.
- [47] Chen, D.; Wang, S.; Xiao, M.; Meng, Y. Synthesis and Properties of Novel Sulfonated Poly(Arylene Ether Sulfone) Ionomers for Vanadium Redox Flow Battery. *Energy Convers. Manage.* **2010**, *51* (12), 2816–2824. doi:10.1016/j.enconman.2010.06.019.
- [48] Kim, S.; Tighe, T.B.; Schwenzler, B.; Yan, J.; Zhang, J.; Liu, J.; Yang, Z.; Hickner, M.A. Chemical and Mechanical Degradation of Sulfonated Poly(Sulfone) Membranes in Vanadium Redox Flow Batteries. *J. Appl. Electrochem.* **2011**, *41* (10), 1201–1213. doi:10.1007/s10800-011-0313-0.
- [49] Macksasitorn, S.; Changkhamchom, S.; Sirivat, A.; Siemanond, K. Sulfonated Poly(Ether Ether Ketone) and Sulfonated Poly(1,4-Phenylene Ether Ether Sulfone) Membranes for Vanadium Redox Flow Batteries. *High Perform. Polym.* **2012**, *24* (7), 603–608. doi:10.1177/0954008312446762.
- [50] Chen, D.; Hickner, M.A. V<sup>5+</sup> Degradation of Sulfonated Radel Membranes for Vanadium Redox Flow Batteries. *Phys. Chem. Chem. Phys.* **2013**, *15* (27), 11299. doi:10.1039/c3cp52035h.
- [51] Choi, S.-W.; Kim, T.-H.; Jo, S.-W.; Lee, J.Y.; Cha, S.-H.; Hong, Y.T. Hydrocarbon Membranes with High Selectivity and Enhanced Stability for Vanadium Redox Flow Battery Applications: Comparative Study with Sulfonated Poly(Ether Sulfone)s and Sulfonated Poly(Thioether Ether Sulfone)s. *Electrochim. Acta* **2018**, *259*, 427–439. doi:10.1016/j.electacta.2017.10.121.
- [52] Herrmann, E.; Dingenouts, N.; Roth, C.; Scheiba, F.; Ehrenberg, H. Systematic Characterization of Degraded Anion Exchange Membranes Retrieved from Vanadium Redox Flow Battery Field Tests. *Membranes*. **2021**, *11* (7), 469. doi:10.3390/membranes11070469.
- [53] Xing, Y.; Liu, L.; Wang, C.; Li, N. Side-Chain-Type Anion Exchange Membranes for Vanadium Flow Battery: Properties and Degradation Mechanism. *J. Mater. Chem. A* **2018**, *6* (45), 22778–22789. doi:10.1039/C8TA08813F.
- [54] Yuan, Z.; Li, X.; Zhao, Y.; Zhang, H. Mechanism of Polysulfone-Based Anion Exchange Membranes Degradation in Vanadium Flow Battery. *ACS Appl. Mater. Interfaces* **2015**, *7* (34), 19446–19454. doi:10.1021/acsami.5b05840.
- [55] Jung, M.J.; Parrondo, J.; Arges, C.G.; Ramani, V. Polysulfone-Based Anion Exchange Membranes Demonstrate Excellent Chemical Stability and Performance for the All-Vanadium Redox Flow Battery. *J. Mater. Chem. A* **2013**, *1* (35), 10458.
- [56] Yue, M.; Zhang, Y.; Wang, L. Sulfonated Polyimide/Chitosan Composite Membrane for Vanadium Redox Flow Battery: Influence of the Infiltration Time with Chitosan Solution. *Solid State Ionics* **2012**, *217*, 6–12. doi:10.1016/j.ssi.2012.04.003.
- [57] Charyton, M.; Deboli, F.; Fischer, P.; Henrion, G.; Etienne, M.; Donten, M.L. Composite Anion Exchange Membranes Fabricated by Coating and UV Crosslinking of Low-Cost Precursors Tested in a Redox Flow Battery. *Polymers. (Basel)* **2021**, *13* (15), 2396. doi:10.3390/polym13152396.
- [58] Gong, K.; Fang, Q.; Gu, S.; Li, S.F.Y.; Yan, Y. Nonaqueous Redox-Flow Batteries: Organic Solvents, Supporting Electrolytes, and Redox Pairs. *Energy Environ. Sci.* **2015**, *8* (12), 3515–3530. doi:10.1039/C5EE02341F.
- [59] Kowalski, J.A.; Su, L.; Milshtein, J.D.; Brushett, F.R. Recent Advances in Molecular Engineering of Redox Active Organic Molecules for Nonaqueous Flow Batteries. *Curr. Opin. Chem. Eng.* **2016**, *13*, 45–52. doi:10.1016/j.coche.2016.08.002.
- [60] Tang, L.; Leung, P.; Xu, Q.; Mohamed, M.R.; Dai, S.; Zhu, X.; Flox, C.; Shah, A.A. Future Perspective on Redox Flow Batteries: Aqueous Versus Nonaqueous Electrolytes. *Curr. Opin. Chem. Eng.* **2022**, *37*, 100833. doi:10.1016/j.coche.2022.100833.
- [61] Takechi, K.; Kato, Y.; Hase, Y. A Highly Concentrated Catholyte Based on a Solvate Ionic Liquid for Rechargeable Flow Batteries. *Adv. Mater.* **2015**, *27* (15), 2501–2506. doi:10.1002/adma.201405840.
- [62] Cong, G.; Zhou, Y.; Li, Z.; Lu, Y.-C. A Highly Concentrated Catholyte Enabled by a Low-Melting-Point Ferrocene Derivative. *ACS Energy Lett.* **2017**, *2* (4), 869–875. doi:10.1021/acseenergylett.7b00115.
- [63] Chen, H.; Cong, G.; Lu, Y.-C. Recent Progress in Organic Redox Flow Batteries: Active Materials, Electrolytes and Membranes. *J. Energy Chem.* **2018**, *27* (5), 1304–1325. doi:10.1016/j.jechem.2018.02.009.